BIOCHEMISTRY
including biophysical chemistry & molecular biology

Article

pubs.acs.org/biochemistry

Impact of pH on the Structure and Function of Neural Cadherin

Jared M. Jungles, Matthew P. Dukes, Nagamani Vunnam, and Susan Pedigo*

Department of Chemistry and Biochemistry, University of Mississippi, University, Mississippi 38677, United States

Supporting Information

ABSTRACT: Neural (N-) cadherin is a transmembrane protein within adherens junctions that mediates cell−cell adhesion. It has 5 modular extracellular domains (EC1−EC5) that bind 3 calcium ions between each of the modules. Calcium binding is required for dimerization. N-Cadherin is involved in diverse processes including tissue morphogenesis, excitatory synapse formation and dynamics, and metastasis of cancer. During neurotransmission and tumorigenesis, fluctuations in extracellular pH occur, causing tissue acidosis with associated physiological consequences. Studies reported here aim to determine the effect of pH on the dimerization properties of a truncated construct of N-cadherin containing EC1−EC2. Since N-cadherin is an anionic protein, we hypothesized that acidification of solution would cause an increase in stability of the apo protein, a decrease in the calcium-binding affinity, and a concomitant decrease in the formation of adhesive dimer. The stability of the apo monomer was increased and the calcium-binding affinity was decreased at reduced pH, consistent with our hypothesis. Surprisingly, analytical SEC studies showed an increase in calcium-induced dimerization as solution pH decreased from 7.4 to 5.0. Salt-dependent dimerization studies indicated that electrostatic repulsion attenuates dimerization affinity. These results point to a possible electrostatic mechanism for moderating dimerization affinity of the Type I cadherin family. Extrapolating these results to cell adhesion in vivo leads to the assertion that decreased pH promotes adhesion by N-cadherin, thereby stabilizing synaptic junctions.

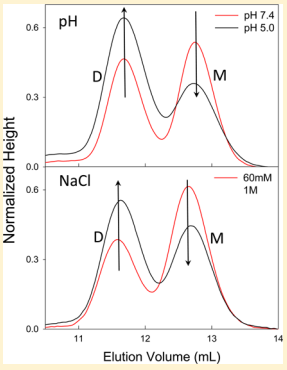

Extracellular pH in humans is actively maintained between pH 7.2 and 7.4, except in abnormal states such as metastatic cancer,[1,2] diabetic ketoacidosis,[3] high levels of lactate,[4] critical illness,[5] and in normal and diseased brain tissue where the pH decreased to between 6.8[6,7] and 6.2.[8] The effect of the microenvironment on cell−cell adhesion may play a significant physiological role in the stability of adherens junctions and the associated intracellular events. Our interest is in how decreased pH will affect adhesion by N-cadherin, a cell adhesion molecule in adherens junctions that is critical in neurological synapse formation.[9,10] N-Cadherin is the primary cell adhesion protein within synaptic adherens junctions at the transmission zone and is directly exposed to proton flux during periods of increased synaptic activity.[11] N-Cadherin expression is also up-regulated in tumor progression, angiogenesis, and metastasis of numerous types of cancer cells.[12−15] Tumors in active periods of growth have been shown to acidify due to the Warburg effect, a state that is consistent with tumor cell proliferation.[16,17] Since N-cadherin is an anionic protein that requires calcium binding for proper function, pH may have a profound effect on its structure, stability, and function.

N-Cadherin is a member of the classical or type I cadherin family consisting of five tandem repeating extracellular domains, a single-pass transmembrane region, and a conserved C-terminal cytoplasmic region. Formation of adhesive dimers between cadherins on apposing cell surfaces occurs through the formation of a strand-swapped structure, which forms via the exchange of the N-terminal βA-strand between juxtaposed EC1 domains. The strand-swapped structure is stablilized by docking of the side chain of a conserved tryptophan (W2) into the conserved hydrophobic pocket of the neighboring protomer (c.f., ref 18). Since the strand-swapped interface is located in the first domain of the EC region,[19,20] the studies reported herein utilize the first two EC-domains of N-cadherin (NCAD12). The two-domain construct has been well characterized in Type I cadherins[18,21,22] and is the minimal functional unit required for calcium-dependent dimerization in vitro.

The interface between tandem EC domains contains amino acids that play critical roles in the adhesion process. Calcium-binding sites comprise clusters of negatively charged carboxyl groups from both modular domains at the interdomain interface. The critical anionic residues in the NCAD12 calcium-binding pocket are E11, D67, E69, D103, D134, D136, and D194 in N-cadherin. Calcium-binding sites 1 and 2 are linked by the side chain oxygens of E11, E69, and D103. Sites 2 and 3 are linked by the side chain oxygens of D136, while site 3 comprises, in part, both side chain oxygens from D134.[21] Studies have shown that mutations of these residues resulted in a dramatic decrease in calcium-binding affinity and dimerization.[23−26]

Isolated amino acid pK_a values of acidic residues (4.5−3.3) are well outside the physiologicially relevant range (7.4−6.0);[27] however, pK_a values for acidic residues in folded proteins can differ by orders of magnitude from these canonical values, especially in acidic proteins where they have been shown to be

Received: August 26, 2014
Revised: November 1, 2014
Published: November 3, 2014

   dx.doi.org/10.1021/bi5010798 | *Biochemistry* 2014, 53, 7436−7444

as high as 9.[28−30] NCAD12 also contains three histidine residues (H75, H79, and H110) whose protonation state may change in a physiological relevant pH range. Histidine residues have been characterized as "pH sensors",[31−33] whose protonation state can affect protein conformational stability in a physiological pH range.[34] Thus, we might expect significant protonation of critical acidic and histidine residues in a physiologically relevant pH range.

Since the residues comprising the calcium binding sites are highly anionic, we propose that a decrease in solution pH should stabilize NCAD12 due to the decrease in electrostatic repulsion from neutralization of acidic residues. We also propose that an increase in solution acidity should introduce competition between calcium and protons for site occupancy, resulting in a reduction of calcium-binding affinity followed by a concomitant decrease in dimerization affinity. In this work, we address the impact of pH on the stability, calcium-binding affinity, and the dimerization affinity of NCAD12 protomers using spectroscopic and chromatographic methods.

EXPERIMENTAL PROCEDURES

Protein Expression and Purification. The cloning of the gene for the first two extracellular domains (residues 1−221) of NCAD12 (EC1, linker1, EC2, and linker2) was described previously.[35] Recombinant pET30 Xa/LIC plasmids were amplified by KOD HiFi DNA Polymerase (Stratagene) and transformed into *Escherichia coli* BL21 (DE3) cells.[35] Protein was overexpressed and purified as described in previous work.[26] Protein purity was verified via SDS-PAGE in 17% Tris-Glycine gels through standard protocols. The concentration of the protein stocks was determined spectrophotometrically (ε_{280} = 15 900 ± 400 M^{-1} cm^{-1}).[36]

Dilution Method for pH Adjustment. In order to create protein solutions over a range of pHs (7.4−5.0), we prepared our stock at pH 7.4, but with a low buffer strength (2 mM HEPES). Identical diluent buffers at higher buffer strength were made at pHs 7.4, 7.0, and 6.5 (40 mM HEPES, 140 mM NaCl) and at pH 6.0, 5.5, and 5.0 (40 mM NaOAc, 140 mM NaCl). The NCAD12 stock in 2 mM HEPES at pH 7.4 was diluted 1 part protein stock plus 2.4 parts diluent buffer (e.g., 80 μM stock; 23.5 μM working concentration). We confirmed that this dilution ratio was sufficient to adjust the pH to the desired level by measuring pH with a microelectrode.

Thermal Unfolding Studies. Thermal unfolding studies as a function of calcium and pH (6.0, 6.5, 7.0, and 7.4) were performed on an AVIV 202SF Circular Dichroism (CD) Spectrometer. Solutions of 5 μM NCAD12 were placed in a 1 cm quartz cuvette with a fitted temperature probe inserted through the stopper. This concentration was chosen to minimize dimer formation while maximizing signal-to-noise. The solution was stirred throughout data acquisition. Data were acquired at 227 nm at a temperature range of 15−95 °C (1 °C intervals with a 30 s equilibration period and a 5 s data averaging time). Thermal denaturation profiles were identical with expanded equilibration times (30 s to 2 min) during data acquisition indicating that the kinetics of unfolding were rapid (Supporting Information). The calcium-saturated samples were brought to 2.5 mM total calcium concentration to ensure maximum saturation of binding sites at all pH values. Data were fit to the Gibbs−Helmholtz equation with linear native and denatured baselines as described previously.[37] T_m and ΔH_m values were allowed to vary in fits to this equation, while ΔC_p was fixed to 1 kcal mol^{-1} K^{-1}.[35] ΔC_p was also fixed to 0 kcal mol^{-1} K^{-1} and 2 kcal mol^{-1} K^{-1} to determine the effect of its value on resolved values of ΔH_m and T_m. Variation in resolved parameters, as a function of the value for ΔC_p, was smaller than the standard deviation in the resolved parameters. Thermal denaturation is a reversible process in NCAD12; however, refolding is slower than unfolding, likely due to the abundance of prolines in the protein.[38]

Calcium Titrations. The CD signal of NCAD12 was monitored during calcium titrations using an Olis DSM 20 CD Spectrometer. Solutions of 1, 10, 100, and 700 mM $CaCl_2$ were each added sequentially in 2.5, 5.0, and 10.0 μL increments to 5 μM NCAD12 in solutions with pH values between 7.4 and 5.5. Samples were stirred throughout the titration. Titrations were performed at least twice. CD signal was recorded in wavelength scans from 300 to 210 nm with an averaging time (1−13 s) that was proportional to dynode voltage at each wavelength. To resolve free energy changes for calcium binding, titration data were considered at wavelengths from 230 to 220 nm to optimize the signal-to-noise ratio. Titration data were fit to an equation for equal and independent sites with linear apo and saturated baselines. While we expected cooperative binding of calcium, data did not support analysis by a more complex model based on the span and randomness of residuals of fitted data.

In order to determine the apparent pK_a for the protonation event(s) that affected calcium binding affinity, we used a simple competitive model as described by the equations below

$$\frac{K_X \cdot X \cdot M_o \cdot (Z)}{1 + K_X \cdot X \cdot (Z)} = MX \tag{1}$$

$$Z = \left(1 - \frac{K_Y \cdot Y}{1 + K_Y \cdot Y}\right) \tag{2}$$

where M_o is the total protein concentration, X is the concentration of calcium, and Y is the concentration of protons. K_x is the association constant for calcium and K_y is the association constant for protons. Prior to analysis data were normalized to end points from individual fits, and then end points were fixed in the global analysis to determine the values of K_x and K_y.

Disassembly and Assembly Studies. The impact of pH on dimer formation was investigated using size exclusion chromatography (SEC). A Superose-12 10/300 GL column (Amersham) was used on an ÄKTA Purifier HPLC system (Amersham) with UV absorbance detection at 280 nm, a 0.5 mL/min flow rate, and a 75 μL injection volume. The mobile phase consisted of 10 mM HEPES, 140 mM NaCl, pH 7.4 (SEC Buffer). Chromatograms were offset corrected and then normalized against the sum of the heights of the monomer and dimer peaks in the pH 7.4 sample to correct for small differences in injection volume. Elution volumes of monomer and dimer peaks were determined to have a precision of ±0.04 mL in single day, and ±0.06 mL between days.

To determine the effect of pH on the assembly of dimer in the presence of calcium, we exploited an analytically useful property of NCAD12. That is, rapid decalcification of the calcium-saturated NCAD12 dimer (D_{sat}) causes the formation of a kinetically trapped dimer (D^*_{apo}). In this method, the concentration of D^*_{apo} reflects the amount of D_{sat} in the calcium-saturated solution.[26] To measure the effect of pH on the formation of D_{sat}, we first assessed the effect of pH on D^*_{apo}. Second, we determined the effect of pH on D_{sat}.

dx.doi.org/10.1021/bi5010798 | *Biochemistry* 2014, 53, 7436−7444

Table 1. Results from Thermal Denaturation Experiments

buffer	ΔH_m (kcal/mol)	T_m (°C)	$\Delta G°^b$ (kcal/mol)	ΔH_m (kcal/mol)	T_m (°C)	$\Delta G°^b$ (kcal/mol)
pH 7.4	74 ± 3	44.0 ± 0.1	1.6 ± 0.2	90 ± 3	56.6 ± 0.1	4.8 ± 0.2
pH 7.0	71 ± 3	44.7 ± 0.2	1.6 ± 0.1	91 ± 5	56.3 ± 0.2	4.8 ± 0.1
pH 6.5	71 ± 3	46.0 ± 0.2	1.9 ± 0.2	94 ± 2	56.2 ± 0.1	4.9 ± 0.2
pH 6.0	67 ± 2	48.5 ± 0.5	2.2 ± 0.2	N/A[c]	N/A[c]	N/A[c]

[a]Gibbs–Helmholtz equation where ΔC_p was fixed at 1 kcal mol^{-1} K^{-1}.[35] Reported errors were resolved from global analysis of replicate experiments. [b]Values were calculated at 37 °C. [c]Values were not resolved due to protein precipitation.

To determine if pH had an effect on the disassembly of D^*_{apo}, the protein stock (80 μM, pH 7.4) was brought to 1 mM calcium concentration and incubated for 5 min before adding EDTA (5 mM, 30 min incubation time) to decalcify and convert D_{sat} to D^*_{apo}. The dilution method outlined above was used to bring the protein to a desired pH, and samples were injected on the SEC column equilibrated in SEC buffer (pH 7.4) to assess the level of monomer and dimer. To observe if disassembly of D^*_{apo} was time dependent, samples were incubated after dilution to the desired pH for 0, 1, and 5 h before injecting on the column.

To assess whether pH had an effect on the level of D_{sat}, we first established that D^*_{apo} did not disassemble at pHs lower than 7.4. Then, we prepared protein samples using the dilution method outlined above in the presence of 1 mM calcium, added EDTA (5 mM) to convert D_{sat} to D^*_{apo}, and injected the samples on the SEC column. The protein solutions were at final pH values of 5.0, 5.5, 6.0, 6.5, 7.0, and 7.4.

To determine if the concentration of NaCl would impact the formation of D_{sat}, the previous experiment was performed in buffers with 60, 140, 500, 750, and 1000 mM NaCl at pH 7.4. Samples with greater than 140 mM NaCl were prepared by adding concentrated NaCl solutions to the protein stock. Samples at each NaCl concentration were then brought to 1 mM calcium concentration and incubated for 5 min followed by addition of 5 mM EDTA and then injection on the SEC column.

Prediction of pK_a Values. To estimate the pK_a of titratable residues, we used PROPKA (3.1). It uses a five-stage empirical computing algorithm that accounts for the effects of hydrogen bonding, charge–charge interactions, and desolvation from structural data resulting in predicted pK_a values with an overall RMSD of 0.79 pH units from experimental studies.[39−42] PROPKA predicted the charge of NCAD12 as −8.8 at pH 7.0. pK_a values were predicted for all ionizable residues in NCAD12 with calcium ions present in 2QVI.pdb. The 2QVI structure with calcium ions removed was not further minimized. According to PROPKA 3.1, the pI of NCAD12 is pH 4.3.

Distances between residues in 2QVI crystal structure were determined with Swiss-Pdb Viewer.[43−45] Distances mentioned were from the terminal carbon of each residue's side chain to illustrate distance between charged portions of each side chain, e.g., carboxyl group of D27 to carboxyl group of E89.

RESULTS

Thermal Unfolding Studies. Thermal unfolding studies were performed to observe the impact of pH and calcium on the stability of NCAD12. The CD signal was monitored as a function of temperature. Two distinct transitions were observed with the signal becoming increasingly negative as the protein unfolded, consistent with a polyproline conformation of the unfolded state.[46] Raw CD thermal denaturations are shown in Supporting Information. Previous work has shown that the first transition corresponds to unfolding of EC2 and the second transition to unfolding of EC1.[47] In the absence of calcium, NCAD12 was soluble and monomeric (M_{apo}) from pH 7.4 to 6.0. NCAD12 precipitated during denaturation experiments at pH values approaching its pI, so we were unable to obtain estimates of stability at pH values below 6.0 in the apo state and below 6.5 in the calcium-saturated state (M_{sat}). In the apo-state, the apparent stability of the protein increased as pH decreased. Data for the first transition were fit to the Gibbs–Helmholtz equation with adjustable baseline parameters. Fitting of the first transition is represented in SI Figure A. The values resolved for T_m increased significantly as the pH decreased while the values resolved for ΔH_m decreased slightly leading to a net increase in calculated values for $\Delta G°$ at 37 °C (Table 1). As expected, the stability of NCAD12 (EC2) increased in the presence of calcium (Figure 1). In the presence of calcium, the thermal-

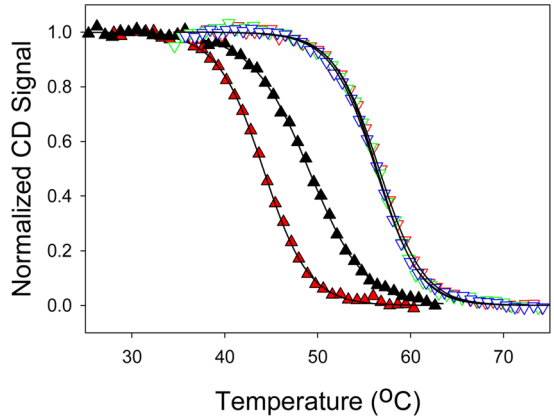

Figure 1. Thermal denaturation of NCAD12 as a function of pH and calcium. In the apo-state, data for the first unfolding transition of NCAD12 at pH 7.4 (red) and 6.0 (black) are shown (closed). In the calcium saturated state data are shown (open) at pH 7.4 (red), 7.0 (green), and 6.5 (blue). CD signal at 227 nm is reported. Solid lines are simulated based on parameters resolved from the Gibbs–Helmholtz equation. Resolved Free energy values are given in Table 1.

denaturation profiles were indistinguishable over the accessible pH range. Identical values resolved for T_m, ΔH_m, and calculated values for $\Delta G°$ at 37 °C indicate that the binding of calcium masked the effect of decreased pH that was observed in the apo state. Analysis of the second transition (unfolding of EC1) was problematic due to protein precipitation at pH 7.0 or less at temperatures at which the EC1 transition was occurring.

Calcium Titrations. The pH dependence of calcium-binding affinity of NCAD12 was assessed via calcium titrations monitored by CD spectroscopy. Figure 2A shows the CD signal as a function of calcium concentration at each pH. The data at each pH were normalized to correct for the pH dependence of the magnitude of the CD signal, and then offset for clarity. The CD signal increased (less negative) with the addition of calcium

dx.doi.org/10.1021/bi5010798 | Biochemistry 2014, 53, 7436−7444

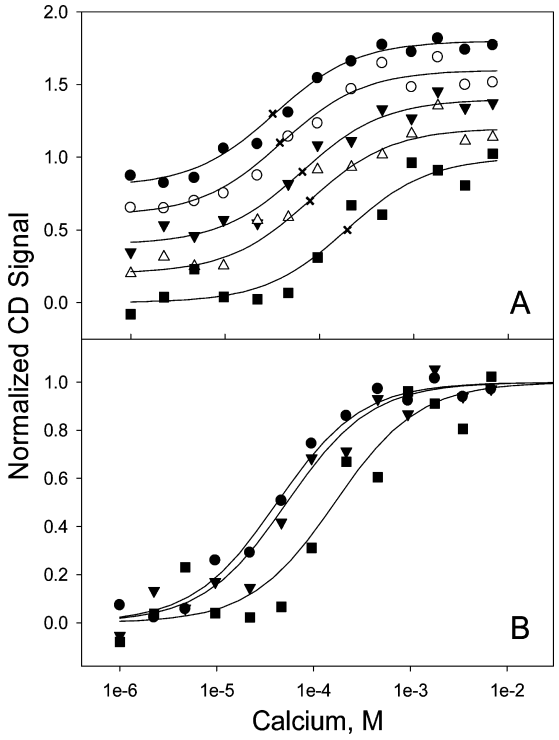

Figure 2. Calcium titrations of NCAD12 as a function of pH. NCAD12 was titrated with calcium at pH 7.4 (●), 7.0 (○), 6.5 (▼), 6.0 (Δ), and 5.5 (■); the normalized CD signal is plotted against total calcium concentration. (A) Representative titrations at each pH are shown. Solid lines are simulated based on parameters resolved from global analysis of at least two separate experiments. Data are normalized and offset for clarity. Midpoints of transitions are designated by X. (B) To resolve the pK_a of the protonation event that impacted the apparent calcium binding affinity at each pH, data were analyzed according to a competitive binding model. Resolved values for the changes in free energy of binding are shown in Table 2.

at all pH values consistent with calcium-induced changes in structure. Since the span of the CD signal over the course of titrations performed at pH 6.0 and 5.5 was low ($\Delta\Delta\varepsilon$ 2.3 ± 0.3 mdeg), the signal-to-noise ratio was poor. Studies were also attempted at pH 5.0; however, protein precipitated during the titration. NCAD12 was >85% saturated at 1 mM Ca^{2+} at all pH values.

Based on the randomness and span of residuals, data fitted well to a binding model of equal and independent sites indicating that there was no observed cooperativity in calcium binding from pH 7.4 to 5.5. There was a small, yet systematic, decrease in calcium-binding affinity as pH decreased from 7.4 to 6.0 with a significant decrease in affinity as the pH was decreased further to 5.5. This pH-dependent difference is reflected in resolved values for K_a in Table 2 ($K_{a7.4} = 3{\cdot}K_{a6.0}$, and $K_{a6.0} = 3{\cdot}K_{a5.5}$).

Proton binding decreases the apparent calcium binding constant (Table 2). In order to estimate the pK_a of the relevant protonation event(s), calcium binding data as a function of pH were fit to a competitive binding model given in eqs 1 and 2. Data at all pH values were simultaneously analyzed to determine the binding constants for calcium and protons. Resolved values are in Table 2. The K_a for calcium from individual analysis of data at pH 7.4 was similar to that found from analysis of calcium binding data at pH 7.4, the reference pH for the experiments presented here. The apparent pK_a (log of the association constant for protons) for the proton binding event(s) that perturbs calcium binding is 6.0 ± 0.1, a value close to the canonical value for histidine or an acidic residue such as aspartate or glutamate.

Table 2. Free Energies of Calcium Binding Resolved from Analysis of Calcium Titrations

individual analysis[a]	
pH	K_a
7.4	(35 ± 10) × 10^3
7.0	(25 ± 8) × 10^3
6.5	(18 ± 7) × 10^3
6.0	(13 ± 6) × 10^3
5.5	(4.7 ± 1.4) × 10^3
competitive model[b]	
$K_a(Ca^{2+})$	(25 ± 3) × 10^3
$K_a(H^+)$	(10 ± 3) × 10^5
pK_a[c]	(6.0 ± 0.1)

[a]Apparent association constants for calcium from analysis of data at each pH independently. [b]Fits of data to eqs 1 and 2 yielding apparent association constants for calcium ions and protons. [c]pK_a value is the log of the proton association constant.

Disassembly/Assembly Studies. Analytical size-exclusion chromatography (SEC) was performed to monitor the level of formation of calcium-saturated, adhesive dimer (D_{sat}) as a function of pH. We first investigated the effect of pH on the disassembly of D^*_{apo} (Figure 3A). The dimer eluted at 11.72 ± 0.04 mL and the monomer at 12.82 ± 0.04 mL. Previous studies of this system found that these retention volumes correspond to the calculated radius of gyration based on the crystal structures of the monomeric and strand-swapped dimer structures for classical cadherins.[35] As pH decreases over a range from pH 7.4 to 5.0, there is no change in the percentage of dimer (χ_D) in the sample, indicating that D^*_{apo} remained kinetically trapped. To determine if the disassembly of D^*_{apo} at low pH was time dependent, protein stock at pH 7.4 was diluted to low pH and incubated for 1 and for 5 h before chromatographic analysis. The level of D^*_{apo} in those experiments did not change over the 5 h time period (χ_D = 51 ± 1%; data not shown). It was determined that a decrease in pH did not disassemble D^*_{apo}.

We monitored the level of D_{sat} by adjusting the sample to the desired pH, adding calcium to form D_{sat}, then EDTA to convert D_{sat} to D^*_{apo} for quantification via analytical SEC. This chromatographic experiment provided a "snapshot" of the level of D_{sat} at a particular pH and concentration. Unexpectedly, with a decrease in pH, we observed an increasing trend in the fraction saturated dimer (χ_D) from 0.49 at pH 7.4 to 0.53 at pH 6.0 (Table 3). In this chromatographic experiment we were able to broaden our pH window to 5.0 without protein precipitation and found that χ_D continued to increase to 0.65 at pH 5.0. Representative size exclusion chromatograms are shown in Figure 3B, and illustrate the level of D_{sat} in solution as a function of pH. Contrary to our expectations, the level of D_{sat} systematically increased with a change in pH from 7.4 to 5.0. These results imply that the dimerization of NCAD12 increased with a decrease in pH due to protonation of acidic or histidine residues.

The increase of dimer to monomer ratio as a function of pH led us to study the effect of salt concentration on dimerization. Again, we used the level of D^*_{apo} in calcium-depleted samples to monitor the level of D_{sat} in 1 mM calcium as a function of

dx.doi.org/10.1021/bi5010798 | Biochemistry 2014, 53, 7436−7444

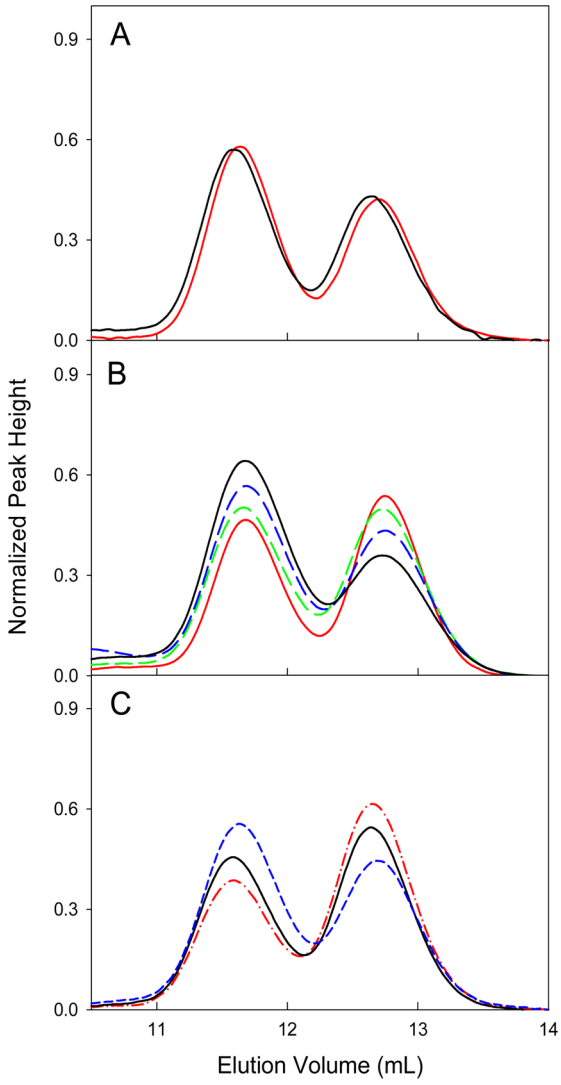

Figure 3. Analytical SEC chromatograms to assess the impact of pH on (A) the disassembly of D^*_{apo} (A) at pH 7.4 (red) and pH 6.0 (black), and on (B) the assembly of D_{sat} at pH 7.4 (red), pH 6.0 (green), pH 5.5 (blue), and pH 5.0 (black). (C) Analytical SEC chromatograms to assess the impact of NaCl concentrations at 60 mM (red), 140 mM (black), and 1 M (blue) on the assembly of D_{sat}. *Y*-axis was normalized based on the heights of the monomer and dimer peaks. Apparent dissociation constants are in Table 3.

Table 3. Results from Analytical SEC for the Assembly of the Calcium-Saturated Dimer

pH	K_d (μM)	χ_D	[NaCl] mM	K_d (μM)	χ_D
7.4	25 ± 3	0.49 ± 0.03	60	40 ± 1	0.39 ± 0.01
7.0	23 ± 4	0.50 ± 0.03	140	31 ± 5	0.45 ± 0.04
6.5	21 ± 2	0.52 ± 0.02	500	23 ± 2	0.48 ± 0.01
6.0	20 ± 2	0.53 ± 0.03	750	21 ± 3	0.50 ± 0.02
5.5	14 ± 1	0.58 ± 0.01	1000	13 ± 2	0.57 ± 0.02
5.0	9 ± 1	0.65 ± 0.01			

the NaCl concentration. Dimer formation was found to increase with an increase in NaCl concentration (Figure 3C). Dissociation constants and fraction saturated dimer percentages were calculated at all pH values and salt concentrations (Table 3). Retention volume of the larger species (dimer peak) at low pH was consistent with the predicted radius of gyration of the dimer, a size well within the working range of the SEC column.

Prediction of pK_a Values in NCAD12. NCAD12 is an acidic protein with 26 acidic residues and 19 basic residues, including 3 histidines. The results from PROPKA 3.1 computations of pK_a values for selected residues in the presence of calcium ions are shown in Table 4. Residues that have high accessible surface area generally have computed pK_a values close to the canonical values as typified by E20, E181, H75, and H110. His 79 is located near (~10 Å) the strand-swapped interface in EC1, and is only 26% exposed leading to a slightly depressed pK_a as one would expect for a buried basic residue. All acidic residues with <50% ASA are associated with the calcium binding sites; their pK_a values are harder to predict, a phenomenon that is well documented for acidic residues in active sites[48] or buried in the interior of proteins.[49] Several buried calcium-binding residues (E11 (pK_a 7.5) and D134 (pK_a 6.2))[18] are predicted to have pK_a values significantly more basic than canonical values and are, therefore, titratable in a physiological range of pH.

Table 4. Results from PROPKA Predictions

residue	predicted pK_a[a]	model pK_a	%ASA[b]
D27[c]	4.0	3.8	73
D29	2.5	3.8	32
D67[d]	1.3	3.8	36
D93[c]	3.7	3.8	59
D103[d]	2.3	3.8	31
D134[d]	6.2	3.8	1
D136[d]	3.2	3.8	0
D194[d]	3.6	3.8	0
E11[d]	7.5	4.5	0
E20[c]	4.6	4.5	87
E69[d]	4.7	4.5	18
E89	3.3	4.5	36
E119	5.9	4.5	28
H75[c]	6.1	6.1	61
H79	5.7	6.1	26
H110[c]	6.3	6.1	67

[a]Calcium ions retained in 2QVI structure. [b]Percent accessible surface area according to Get Area.[73] [c]Surface exposed residues, not involved in binding calcium. [d]Calcium-binding residues.

DISCUSSION

N-Cadherin, a member of the classical cadherin family, is an acidic protein that requires calcium for its function as a primary cell−cell adhesion molecule in adherens junctions. It plays pivotal roles in tissue development,[50,51] cancer,[12,15,52] and neurological synapses.[53,54] Due to its prominent physiological role, the structure−function relationship of N-cadherin has been of interest recently. In particular, our laboratory is interested in the effect of microenvironment on the adhesive properties of N-cadherin. Given the fact that key physiological processes cause acidification of tissue, studies reported herein assess the effect of pH on N-cadherin function. Since we expected that protonation of calcium-binding residues would decrease calcium-binding affinity, and calcium binding is required for dimerization, then it follows that dimerization affinity should also decrease. Surprisingly, a decrease in pH promoted dimerization. In the following discussion, we discuss

dx.doi.org/10.1021/bi5010798 | Biochemistry 2014, 53, 7436−7444

the pH dependence of the linkage between stability, calcium-binding affinity, and dimerization.

At pH 7.0, NCAD12 has a predicted net charge of −8.8 in the native state (PROPKA 3.1), consistent with a significant impact of electrostatic repulsion in protein stability. Since a decrease in pH will lead to a net decrease in negative charge, we hypothesized that a decrease in pH should increase the stability of M_{apo}. This phenomenon was indeed observed in thermal denaturation studies and supported by studies from our laboratory. Previous studies on the stability of isolated EC2 modules, from both E-cadherin[55] and N-cadherin,[56] demonstrated that EC2 is destabilized by flanking acidic linker segments. Furthermore, this destabilization by the adjacent linker segments was overcome by addition of NaCl. Taken together, our studies indicate that the EC2 domain is destabilized by electrostatic repulsion and can be stabilized by addition of NaCl or reduced pH.

Protonation leads to a decrease in overall negative charge due to an increase in positive charge on histidines and a decrease in negative charge on acidic residues in N-cadherin. The observed increase in stability in EC2 shown in the thermal-unfolding studies could be due to a combination of protonating histidines and acidic residues. Given the high charge density in the calcium-binding pocket, protonation of calcium-binding residues will also support a net decrease in electrostatic repulsion.

We observed an increase in stabilization of NCAD12 as pH decreased. Thermodynamic parameters in Table 1 provide insight into the increased stabilization of EC2 as a function of pH. Based on earlier studies of isolated EC2 of E-[55] and N-cadherin,[56] we expected to see an increase in T_m and a concomitant increase in the enthalpy change ($\Delta\Delta H_m$) at T_m, as net charge was reduced. However, while T_m increased in these pH-dependent studies, enthalpy decreased, albeit slightly ($\Delta\Delta H_m$ of 7 kcal/mol). Bechtel et al. state that enthalpy of protonation is not a function of pH in studies of protein stability.[57] The linear relationship between ΔH_m and T_m allows prediction of ΔC_p, yielding a ΔC_p for protonation close to 0 kcal/ (mol K). If we consider the increase in T_m, assuming ΔH_m to be constant, it would imply some decrease in entropy at T_m ($T_{m*}\Delta S_m = \Delta H_m$; when ΔH_m is constant). This result indicates that decreasing the pH produces a decrease in conformational entropy, an increased exposure of hydrophobic surface area, or a combination of both.[58] Enthalpy changes for single protonation events of aspartates and glutamates are relatively small compared to those for protein folding (ΔH_p of 0.5 to 1.5 kcal/mol),[59] possibly leading to the small, observed change in the enthalpy of unfolding as a function of pH.

We hypothesized that protonation of acidic residues in the calcium-binding pocket should lead to an overall decrease in the calcium-binding affinity. As predicted, we found that a decrease in pH did decrease calcium-binding affinity; higher calcium levels are required to populate calcium-binding sites at lower pH values. However, the magnitude of this decrease was only a factor of 3 over a 1.5 pH unit range (7.4−6.0). Additional calcium titrations at pH 5.5 showed the same reduction of a factor of 3 over a smaller pH unit range (6.0−5.5), indicating that the protonation of key acidic residues decreases the calcium binding affinity.

Comparison of the paramters resolved from the competitive binding model to the predicted pK_a values of calcium-binding residues (Table 4) indicates that D134 may be the key player in the pH-dependence of calcium binding. This residue in particular is the key requirement for calcium occupancy of the calcium-binding sites.[25,26,60] Our data indicate that when the pH drops below the predicted pK_a for D134, there is a profound impact in the apparent calcium binding constant. Histidine 79 is adjacent to A80 which is in the hydrophobic pocket. Thus, it is also possible that protonation of this residue changes the conformation of the hydrophobic pocket and influences the calcium binding affinity.[61,62]

Our third hypothesis was that the reduction in affinity for calcium will lead to a decreased level of dimerization. Contrary to our expectations, we observed an increase in dimer affinity at the pH values where we observed a decrease in calcium-binding affinity. Salt-dependent studies were performed to confirm that this observation could be explained by an electrostatic affect. The salt-dependent results support the argument that screening of surface charges promotes interaction between protomers, resulting in increased dimer formation. Rakshit et al. suggested that there is an, as yet uncharacterized, intermediate dimeric structure in the transition between X-dimer and strand-swapped dimer structures.[63] This proposed intermediate must bury the strand-swapped interfaces of two protomers since the spectral signal of W2 indicates that it is not exposed to solvent as it undocks and crosses over to dock in a partner protomer in the formation of the strand-swapped dimer. This intermediate implies very close contact between two protomers as the strand-swapped dimer forms. These results imply that charged residues located at the contact surface between protomers at the strand-swapped interface are responsible in tuning dimerization affinity as a function of pH.

Our chromatographic method for assessing the level of D_{sat} requires the use of the kinetically trapped dimer (D^*_{apo}). Previous analytical ultracentrifugation studies showed that D^*_{apo} can be unlocked into fully functional N-cadherin, which eliminates the notion that D^*_{apo} is an indiscriminate aggregate.[35] In addition, D^*_{apo} elutes at the same volume as D_{sat}, supporting the assumption that the structures have the same size.[47] We do not know the structure of D^*_{apo}, but would speculate that it is similar to D_{sat} due to previous studies showing that formation of D^*_{apo} requires W2,[64] an essential residue for adhesive dimer formation (c.f., refs 18,65). In addition, the retention volumes for the salt-dependent studies have the same precision in the measurement of elution volume as do repetitive injections on the same day for all samples indicating that the same structure for D^*_{apo} generated under other conditions such as addition of calcium or low pH. Therefore, from structural and functional work, we can assume that D^*_{apo} is the strand-swapped structure with calcium removed.

Baumgartner et al. recently demonstrated the adhesive properties of N-cadherin are pH dependent in single molecule and cellular interaction studies.[66] They reported a maximal binding activity of N-cadherin at pH 7.4 that decreased significantly over a very narrow pH range to a minimum binding activity at pH 7.0, an opposite trend to the data reported here. While our current report and Baumgartner et al. both study N-cadherin, there are considerable differences in these two studies, including the methods used and the protein constructs studied. Our studies are focused on a minimal functional unit for dimerization that includes only the first two extracellular domains (EC1 and EC2), while Baumgartner et al. studied a 5-domain construct. By considering our studies together, we would conclude that the effect at pH 7.0 reported by Baumgartner et al. must be due to protonation events in EC3−EC5 and impose a dominant negative effect over the pH-

dx.doi.org/10.1021/bi5010798 | Biochemistry 2014, 53, 7436−7444

dependent change in chemistry in EC1 and EC2 reported here. In support, Ozawa et al. highlighted signal transduction through the EC-region of Type I cadherin, and showed that a mutation in the calcium-binding sites between EC2 and EC3 causes a loss of adhesion.[23]

Another important issue with bacterially expressed NCAD12 is the lack of post-translational glycosylation. It has also been shown in the literature that N-glycosylation can affect cadherin stability and adhesive function.[67] Specifically, N-glycosylation in N-cadherin has been shown to increase adhesion.[68] One glycosylation site is located in EC2, while the others are located at points outside of the NCAD12 structure. Furthermore, possible post-translational polysialylation of cadherin as observed for neural cell adhesion molecules (NCAMs) was not possible in the bacterial expression system. Previous studies have demonstrated that the absence of sialic acid modifications on NCAMs result in increased cell adhesion.[69] Both of these modifications should affect the electrostatic surface of N-cadherin, especially the presence of sialic acid.

In conclusion, within the pH range 7.4−5.0 NCAD12 showed a pH-dependent decrease in calcium-binding affinity and increase in dimerization affinity. Since the pH in metatstatic cancers is depressed by up to 1.2 pH units[1,2] as is the pH at neurological synapses,[1,6] we would predict small increases in N-cadherin dimerization affinity. The extracellular neurological microenvironment is complex and dynamic.[70] These microenvironmental factors include local fluxes in calcium concentration[71] and other metals[72] that could compete with the calcium and have a profound affect dimerization by cadherins.

In terms of the structure−function relationship of the classical cadherin family, the change in dimerization affinity is consistent with electrostatic repulsion playing a role in moderating the affinity of dimerization. This observation begs the question of whether electrostatic interactions are definitive contributors to the tuning of the relative affinities of N-, E-, and P-cadherin at the strand-crossover or X-dimer interfaces, thereby playing a role in the equilibria and kinetics of adhesion by classical cadherins.

■ ASSOCIATED CONTENT

Ⓢ Supporting Information

Data are provided that address two aspects of the temperature-induced denaturation studies including the effect of equilibration time at each temperature and the reversibility of the unfolding transition. This material is available free of charge via the Internet at http://pubs.acs.org.

■ AUTHOR INFORMATION

Corresponding Author

*Phone: (662) 915-5328. Fax: (662) 915-7300. E-mail: spedigo@olemiss.edu.

Funding

This work was supported by grant MCB 0950494 from the National Science Foundation.

Notes

The authors declare no competing financial interest.

■ ABBREVIATIONS

Apo, calcium-depleted; CD, circular dichroism; EC, extracellular domain; EC1, extracellular domain 1 of NCAD12; EC2, extracellular domain 2 of NCAD12; EDTA, ethylenediaminetetraacetic acid; HEPES, *N*-(2-hydroxyethyl) piperazine-*N*′-2-ethanesulfonic acid; K_a, acid dissociation constant; K_d, dissociation constant; NaOAc, sodium acetate; NCAD12, neural-cadherin extracellular domains 1 and 2 (residues 1 to 221); PAGE, polyacrylamide gel electrophoresis; SEC, size exclusion chromatography; T_m, melting temperature

■ REFERENCES

(1) Gerweck, L. E., and Seetharaman, K. (1996) Cellular pH gradient in tumor versus normal tissue: potential exploitation for the treatment of cancer. *Cancer Res. 56*, 1194−1198.

(2) Stuwe, L., Muller, M., Fabian, A., Waning, J., Mally, S., Noel, J., Schwab, A., and Stock, C. (2007) pH dependence of melanoma cell migration: protons extruded by NHE1 dominate protons of the bulk solution. *J. Physiol. 585*, 351−360.

(3) Perilli, G., Saracini, C., Daniels, M. N., and Ahmad, A. (2013) Diabetic Ketoacidosis: A Review and Update. *Curr. Emerg. Hosp. Med. Rep. 1*, 10−17.

(4) Adeva-Andany, M., López-Ojén, M., Funcasta-Calderón, R., Ameneiros-Rodríguez, A., Donapetry-García, C., Vila-Altesor, M., and Rodríguez-Seijas, J. (2014) Comprehensive review on lactate metabolism in human health. *Mitochondrion 17*, 76−100.

(5) Fencl, V., Jabor, A., Kazda, A., and Figge, J. (2000) Diagnosis of metabolic acid-base disturbances in critically ill patients. *American Journal of Respiratory and Critical Care Medicine 162*, 2246−2251.

(6) Ziemann, A. E., Allen, J. E., Dahdaleh, N. S., Drebot, II, Coryell, M. W., Wunsch, A. M., Lynch, C. M., Faraci, F. M., Howard, M. A., 3rd, Welsh, M. J., and Wemmie, J. A. (2009) The amygdala is a chemosensor that detects carbon dioxide and acidosis to elicit fear behavior. *Cell 139*, 1012−1021.

(7) Magnotta, V. A., Heo, H. Y., Dlouhy, B. J., Dahdaleh, N. S., Follmer, R. L., Thedens, D. R., Welsh, M. J., and Wemmie, J. A. (2012) Detecting activity-evoked pH changes in human brain. *Proc. Natl. Acad. Sci. U. S. A. 109*, 8270−8273.

(8) Gerweck, L. E., and Seetharaman, K. (1996) Cellular pH gradient in tumor versus normal tissue: potential exploitation for the treatment of cancer. *Cancer Res. 56*, 1194−1198.

(9) Yu, X., and Malenka, R. C. (2004) Multiple functions for the cadherin/catenin complex during neuronal development. *Neuropharmacology 47*, 779−786.

(10) Fannon, A. M., and Colman, D. R. (1996) A model for central synaptic junctional complex formation based on the differential adhesive specificities of the cadherins. *Neuron 17*, 423−434.

(11) Miesenböck, G., De Angelis, D. A., and Rothman, J. E. (1998) Visualizing secretion and synaptic transmission with pH-sensitive green fluorescent proteins. *Nature 394*, 192−195.

(12) Hazan, R. B., Phillips, G. R., Qiao, R. F., Norton, L., and Aaronson, S. A. (2000) Exogenous expression of N-cadherin in breast cancer cells induces cell migration, invasion, and metastasis. *J. Cell Biol. 148*, 779−790.

(13) Gravdal, K., Halvorsen, O. J., Haukaas, S. A., and Akslen, L. A. (2007) A switch from E-cadherin to N-cadherin expression indicates epithelial to mesenchymal transition and is of strong and independent importance for the progress of prostate cancer. *Clin. Cancer Res. 13*, 7003−7011.

(14) Li, G., Satyamoorthy, K., and Herlyn, M. (2001) N-cadherin-mediated intercellular interactions promote survival and migration of melanoma cells. *Cancer Res. 61*, 3819−3825.

(15) Islam, S., Carey, T. E., Wolf, G. T., Wheelock, M. J., and Johnson, K. R. (1996) Expression of N-cadherin by human squamous carcinoma cells induces a scattered fibroblastic phenotype with disrupted cell-cell adhesion. *J. Cell Biol. 135*, 1643−1654.

(16) Warburg, O. (1956) On the origin of cancer cells. *Science 123*, 309−314.

(17) Warburg, O., Wind, F., and Negelein, E. (1927) The metabolism of tumors in the body. *J. Gen. Physiol. 8*, 519−530.

(18) Tamura, K., Shan, W. S., Hendrickson, W. A., Colman, D. R., and Shapiro, L. (1998) Structure-function analysis of cell adhesion by neural (N-) cadherin. *Neuron 20*, 1153−1163.
(19) Boggon, T. J., Murray, J., Chappuis-Flament, S., Wong, E., Gumbiner, B. M., and Shapiro, L. (2002) C-cadherin ectodomain structure and implications for cell adhesion mechanisms. *Science 296*, 1308−1313.
(20) Haussinger, D., Ahrens, T., Aberle, T., Engel, J., Stetefeld, J., and Grzesiek, S. (2004) Proteolytic E-cadherin activation followed by solution NMR and X-ray crystallography. *EMBO J. 23*, 1699−1708.
(21) Nagar, B., Overduin, M., Ikura, M., and Rini, J. M. (1996) Structural basis of calcium-induced E-cadherin rigidification and dimerization. *Nature 380*, 360−364.
(22) Shan, W., Yagita, Y., Wang, Z., Koch, A., Svenningsen, A. F., Gruzglin, E., Pedraza, L., and Colman, D. R. (2004) The minimal essential unit for cadherin-mediated intercellular adhesion comprises extracellular domains 1 and 2. *J. Biol. Chem. 279*, 55914−55923.
(23) Ozawa, M., Engel, J., and Kemler, R. (1990) Single amino acid substitutions in one Ca2+ binding site of uvomorulin abolish the adhesive function. *Cell 63*, 1033−1038.
(24) Pertz, O., Bozic, D., Koch, A. W., Fauser, C., Brancaccio, A., and Engel, J. (1999) A new crystal structure, Ca2+ dependence and mutational analysis reveal molecular details of E-cadherin homoassociation. *EMBO J. 18*, 1738−1747.
(25) Prakasam, A., Chien, Y. H., Maruthamuthu, V., and Leckband, D. E. (2006) Calcium site mutations in cadherin: impact on adhesion and evidence of cooperativity. *Biochemistry 45*, 6930−6939.
(26) Vunnam, N., and Pedigo, S. (2011) Sequential binding of calcium leads to dimerization in neural cadherin. *Biochemistry 50*, 2973−2982.
(27) Creighton, T. E. (1993) *Proteins: structures and molecular properties*, 2nd ed., W. H. Freeman, New York.
(28) Qin, J., Clore, G. M., and Gronenborn, A. M. (1996) Ionization equilibria for side-chain carboxyl groups in oxidized and reduced human thioredoxin and in the complex with its target peptide from the transcription factor NF kappa B. *Biochemistry 35*, 7−13.
(29) Karp, D. A., Gittis, A. G., Stahley, M. R., Fitch, C. A., Stites, W. E., and Garcia-Moreno, E. B. (2007) High apparent dielectric constant inside a protein reflects structural reorganization coupled to the ionization of an internal Asp. *Biophys. J. 92*, 2041−2053.
(30) Karp, D. A., Stahley, M. R., and Garcia-Moreno, B. (2010) Conformational consequences of ionization of Lys, Asp, and Glu buried at position 66 in staphylococcal nuclease. *Biochemistry 49*, 4138−4146.
(31) Rajan, S., Wischmeyer, E., Liu, G. X., Preisig-Müller, R., Daut, J., Karschin, A., and Derst, C. (2000) TASK-3, a novel tandem pore domain acid-sensitive K+ channel an extracellular histidine as pH sensor. *J. Biol. Chem. 275*, 16650−16657.
(32) Gerchman, Y., Olami, Y., Rimon, A., Taglicht, D., Schuldiner, S., and Padan, E. (1993) Histidine-226 is part of the pH sensor of NhaA, a Na+/H+ antiporter in Escherichia coli. *Proc. Natl. Acad. Sci. U. S. A. 90*, 1212−1216.
(33) Fritz, R., Stiasny, K., and Heinz, F. X. (2008) Identification of specific histidines as pH sensors in flavivirus membrane fusion. *J. Cell Biol. 183*, 353−361.
(34) Achilonu, I., Fanucchi, S., Cross, M., Fernandes, M., and Dirr, H. W. (2012) Role of individual histidines in the pH-dependent global stability of human chloride intracellular channel 1. *Biochemistry 51*, 995−1004.
(35) Vunnam, N., Flint, J., Balbo, A., Schuck, P., and Pedigo, S. (2011) Dimeric states of neural- and epithelial-cadherins are distinguished by the rate of disassembly. *Biochemistry 50*, 2951−2961.
(36) Edelhoch, H. (1967) Spectroscopic determination of tryptophan and tyrosine in proteins. *Biochemistry 6*, 1948−1954.
(37) Prasad, A., Housley, N. A., and Pedigo, S. (2004) Thermodynamic stability of domain 2 of epithelial cadherin. *Biochemistry 43*, 8055−8066.
(38) Prasad, A., and Pedigo, S. (2005) Calcium-dependent stability studies of domains 1 and 2 of epithelial cadherin. *Biochemistry 44*, 13692−13701.
(39) Li, H., Robertson, A. D., and Jensen, J. H. (2005) Very fast empirical prediction and rationalization of protein pKa values. *Proteins: Struct., Funct., Bioinf. 61*, 704−721.
(40) Bas, D. C., Rogers, D. M., and Jensen, J. H. (2008) Very fast prediction and rationalization of pKa values for protein−ligand complexes. *Proteins: Struct., Funct., Bioinf. 73*, 765−783.
(41) Søndergaard, C. R., Olsson, M. H., Rostkowski, M., and Jensen, J. H. (2011) Improved treatment of ligands and coupling effects in empirical calculation and rationalization of pKa values. *J. Chem. Theory Comput. 7*, 2284−2295.
(42) Olsson, M. H., Søndergaard, C. R., Rostkowski, M., and Jensen, J. H. (2011) PROPKA3: consistent treatment of internal and surface residues in empirical p K a predictions. *J. Chem. Theory Comput. 7*, 525−537.
(43) Johansson, M. U., Zoete, V., Michielin, O., and Guex, N. (2012) Defining and searching for structural motifs using DeepView/Swiss-PdbViewer. *BMC Bioinformatics 13*, 173.
(44) Guex, N., Peitsch, M. C., and Schwede, T. (2009) Automated comparative protein structure modeling with SWISS-MODEL and Swiss-PdbViewer: A historical perspective. *Electrophoresis 30*, S162−S173.
(45) Schwede, T., Kopp, J., Guex, N., and Peitsch, M. C. (2003) SWISS-MODEL: an automated protein homology-modeling server. *Nucleic Acids Res. 31*, 3381−3385.
(46) Greenfield, N., and Fasman, G. D. (1969) Computed circular dichroism spectra for the evaluation of protein conformation. *Biochemistry 8*, 4108−4116.
(47) Vunnam, N., and Pedigo, S. (2011) Prolines in βA-sheet of neural cadherin act as a switch to control the dynamics of the equilibrium between monomer and dimer. *Biochemistry 50*, 6959−6965.
(48) Nielsen, J. E., and McCammon, J. A. (2003) Calculating pKa values in enzyme active sites. *Protein Sci. 12*, 1894−1901.
(49) Meyer, T., Kieseritzky, G., and Knapp, E. W. (2011) Electrostatic pKa computations in proteins: Role of internal cavities. *Proteins: Struct., Funct., Bioinf. 79*, 3320−3332.
(50) Hatta, K., and Takeichi, M. (1986) Expression of N-cadherin adhesion molecules associated with early morphogenetic events in chick development. *Nature 320*, 447−449.
(51) Inuzuka, H., Redies, C., and Takeichi, M. (1991) Differential expression of R-and N-cadherin in neural and mesodermal tissues during early chicken development. *Development 113*, 959−967.
(52) Mariotti, A., Perotti, A., Sessa, C., and Ruegg, C. (2007) N-cadherin as a therapeutic target in cancer. *Expert Opin. Invest. Drugs 16*, 451−465.
(53) Takai, Y., Shimizu, K., and Ohtsuka, T. (2003) The roles of cadherins and nectins in interneuronal synapse formation. *Curr. Opin Neurobiol 13*, 520−526.
(54) Takeichi, M. (1991) Cadherin cell adhesion receptors as a morphogenetic regulator. *Science 251*, 1451−1455.
(55) Prasad, A., Zhao, H., Rutherford, J. M., Housley, N. A., Nichols, C., and Pedigo, S. (2006) Effect of linker segments upon the stability of epithelial-cadherin domain 2. *Proteins 62*, 111−121.
(56) Vunnam, N., McCool, J. K., Williamson, M., and Pedigo, S. (2011) Stability studies of extracellular domain two of neural-cadherin. *Biochim. Biophys. Acta 14*, 1841−1845.
(57) Becktel, W. J., and Schellman, J. A. (1987) Protein stability curves. *Biopolymers 26*, 1859−1877.
(58) Pace, C. N. (1992) Contribution of the hydrophobic effect to globular protein stability. *J. Mol. Biol. 226*, 29−35.
(59) Kitzinger, C., and Hems, R. (1959) Enthalpies of hydrolysis of glutamine and asparagine and of ionization of glutamic and aspartic acids. *Biochem. J. 71*, 395−400.
(60) Ozawa, M. (2002) Lateral dimerization of the E-cadherin extracellular domain is necessary but not sufficient for adhesive activity. *J. Biol. Chem. 277*, 19600−19608.

(61) Overduin, M., Harvey, T. S., Bagby, S., Tong, K. I., Yau, P., Takeichi, M., and Ikura, M. (1995) Solution structure of the epithelial cadherin domain responsible for selective cell adhesion. *Science 267*, 386−389.
(62) Harrison, O. J., Corps, E. M., and Kilshaw, P. J. (2005) Cadherin adhesion depends on a salt bridge at the N-terminus. *J. Cell Sci. 118*, 4123−4130.
(63) Rakshit, S., Zhang, Y., Manibog, K., Shafraz, O., and Sivasankar, S. (2012) Ideal, catch, and slip bonds in cadherin adhesion. *Proc. Natl. Acad. Sci. U. S. A. 109*, 18815−18820.
(64) Vunnam, N., and Pedigo, S. (2011) Calcium-induced strain in the monomer promotes dimerization in neural cadherin. *Biochemistry 50*, 8437−8444.
(65) Harrison, O. J., Corps, E. M., Berge, T., and Kilshaw, P. J. (2005) The mechanism of cell adhesion by classical cadherins: the role of domain 1. *J. Cell Sci. 118*, 711−721.
(66) Baumgartner, W., Osmanagic, A., Gebhard, M., Kraemer, S., and Golenhofen, N. (2013) Different pH-dependencies of the two synaptic adhesion molecules N-cadherin and cadherin-11 and the possible functional implication for long-term potentiation. *Synapse 67*, 705−715.
(67) Liwosz, A., Lei, T., and Kukuruzinska, M. A. (2006) N-glycosylation affects the molecular organization and stability of E-cadherin junctions. *J. Biol. Chem. 281*, 23138−23149.
(68) Guo, H.-B., Johnson, H., Randolph, M., and Pierce, M. (2009) Regulation of homotypic cell-cell adhesion by branched N-glycosylation of N-cadherin extracellular EC2 and EC3 domains. *J. Biol. Chem. 284*, 34986−34997.
(69) Fujimoto, I., Bruses, J. L., and Rutishauser, U. (2001) Regulation of Cell Adhesion by Polysialic Acid effects on cadherin, immunoglobulin cell adhesion molecule and integrin function and independence from neural cell adhesion molecule biding or signalling activity. *J. Biol. Chem. 276*, 31745−31751.
(70) Marx, G., and Gilon, C. (2012) Molecular basis of memory. *ACS Chem. Neurosci. 12*, 633−642.
(71) Rusakov, D. A., and Fine, A. (2003) Extracellular Ca2+ depletion contributes to fast activity-dependent modulation of synaptic transmission in the brain. *Neuron 37*, 287−297.
(72) Valko, M., Morris, H., and Cronin, M. T. (2005) Metals, toxicity and oxidative stress. *Curr. Med. Chem. 12*, 1161−1208.
(73) Fraczkiewicz, R., and Braun, W. (1998) Exact and efficient calculation of the accessible surface areas and their gradients for macromolecules. *J. Comput. Chem. 19*, 319−333.